Silva Gabreta	vol. 26	p. 99–116	Vimperk, 2020

Dynamics of stand replacing-disturbance and biomass estimation in the Plešné Lake basin

Fluksová Hana [1], **Grill Stanislav** [1], **Bače Radek** [2] **& Hais Martin** [1, *]

[1] *Faculty of Science, University of South Bohemia, Branišovská 1760, CZ-37005 České Budějovice, Czech Republic*
[2] *Faculty of Forestry and Wood Sciences, Czech University of Life Sciences, Kamýcká 1176, CZ-16521 Praha, Czech Republic*
[*] Martin.Hais@prf.jcu.cz

Abstract
Knowledge about forest decay dynamics is important for a better understanding of major forest ecosystem processes. The main aim of this study was to describe the dynamics of the natural decline of a mountain spruce (*Picea abies*) forest caused by bark beetle (*Ips typographus*) infestation in the Plešné Lake basin. Furthermore, we estimated the dry biomass of the trees to get information about wood storage. The spruce forest decay was described in 10 particular years within the period 2000–2015. Individual trees for every year were delineated from aerial photographs to estimate tree position, vitality (healthy, dead, stump) and age class (sapling, young, adult). LiDAR data were acquired (2008, 2011) to estimate tree height, subsequently DBH and volume biomass for 2011 using allometric relationships. At the beginning, in 2000, more than 20 thousand trees were delineated in the basin, where more than 5.8% were dead or dying trees. The strongest bark beetle outbreak occurred prior to 2009, when 74.6% of all trees in the basin were dead. The resulting number of all dead trees was in 2015 67.7%. The average biomass in the basin was 504 t/ha in 2011. The average biomass of particular tree components were 22.4, 26.7, 8.2, 8.6, 294.2, 25.6 and 120.7 t/ha for needles, branch wood, branch bark, fine branches, stem wood, stem bark and roots, respectively.

Key words: Norway spruce, forest decline, biomass estimation

Introduction

Various disturbance types play important roles in forest dynamics and influence tree density, age and species structure (Frelich 2016, Frelich et al. 2018). Every forest disturbance type has its typical consequence for ecosystem integrity. While fire or clear-cutting are connected with rapid damage and/or removal of the canopy and understory forest vegetation (Jean et al. 2019), insect disturbances conserve the dead wood biomass towards decomposition which is an important nutrient source for subsequent forest recovery (Jonášová & Prach 2004). Moreover, defoliation results in increased incoming solar radiation, which supports the growth of seedlings and saplings.

The character of a disturbance can be described with the following parameters – the severity, duration and spatial distribution of the different types of disturbance affecting the

forest (Newton 2007). The severity of an insect forest disturbance is controlled on the one hand by the pest (Wermelinger 2004, Berec et al. 2013), while on the other hand there are many environmental factors (e.g. climate, topography and forest structure) that determine stand susceptibility to the insect affectation (Netherer & Nopp-Mayr 2005, Lausch et al. 2011, Lausch et al. 2013). Moreover the stand susceptibility is also influenced by pre-disturbance long-term stress factors (Hais et al. 2016). Forest disturbances are commonly detected using satellite imagery on the stand level (Cohen et al. 1995), while aerial and UAV imagery (Wang et al. 2004) and LiDAR data (Morsdorf et al. 2004, Vepakomma et al. 2008, Wulder et al. 2012) are used for detection on the tree level.

Forest disturbances influence not only the stand itself but there are many consequences for landscape functioning (Aerts & Honnay 2011). For example, Rozman et al. (2015) and Kopáček et al. (2013) reported the changes in soil and water chemistry after forest decay due to a bark beetle outbreak in the Šumava Mts. Microclimatic change resulting from deforestation is described in many studies based on field measurements (Geiger 2003, Kopáček et al. 2020) or using satellite thermal data (Hais & Kučera 2008). Forest disturbances also have consequences for biodiversity, which can be even increased particularly in the case of natural disturbances (insect outbreaks, fire, windthrows) at the local scale (e.g. Bengtsson et al. 2000, Svoboda et al. 2010).

Although the dynamics of forest decline have been described in many studies (Pickett 1986, Wulder & Franklin 2006), there is a lack of studies focusing on forest disturbance dynamics in relation to dead tree biomass. Dead wood biomass is critical for advanced regeneration in spruce forest and/or creates a basis for natural forest recovery following the forest disturbance (Jonášová & Prach 2004). In our study, we aimed to describe the forest decline due to spruce bark beetle (*Ips typographus* L., 1758) and estimate the biomass volume. The biomass volume presents a reservoir pool for the elements and is necessary for modelling the dynamics of element amounts during the forest decline period. Information about forest biomass can be obtained through different methodological approaches and with different measurements (Newton 2007, Kangas & Maltamo 2009). The volume estimation and tree sampling methods are described in detail in many studies (Köhl et al. 2006, Gregoire & Valentine 2007). Tree biomass (often called wooded biomass) is not only an important factor in biochemical cycles but also serves as a nutrient source for forest recovery (Krankina et al. 1999).

Because of the cost and difficulty of direct field biomass measurements, regression models based on allometric relationships between tree metrics and biomass (Parresol 1999, Repola 2009) or, for larger forest areas, remote sensing and LiDAR scanning techniques (Hauglin et al. 2013, Kankare et al. 2013) are more often used. In this paper, we used aerial photographs and LiDAR data for tree detection and height estimation to calculate biomass using allometric relationships. It corresponds to the main aim of our study, which was to describe the dynamics of forest decline due to bark beetle outbreak and estimate the total biomass of living and dead trees.

Methods

Study area

The study area (Plešné Lake basin) is located in the Šumava Mts. The area belongs to the first natural protected zone in Šumava National Park. Plešné Lake is located at altitudes between 1086–1377 m a.s.l. Total basin area is 63.4 ha including the lake (7.1 ha). An extra 50 m buffer zone surrounding the Plešné Lake basin was added to remove edge effect while calculating the tree density. A small part of the basin (0.5 ha) and part of the buffer zone (1.9 ha) in south west are in Austria. Plešné Lake has a glacial origin which was created partly as a glacial cirque and partly was dammed by a moraine. The basin has a mountainous character with steep slopes (0–86 degrees) and rock forms. The glacier cirque is opened toward the northeast, i.e. slopes around the lake are oriented towards the north, east and south.

Norway spruce (*Picea abies* (L.) Karst.), as the dominant species in the basin (90% area), corresponds to the natural vegetation unit of the basin area (Neuhäuslová et al. 2001). The average stand age was 160 years before disturbance (Svoboda et al. 2006a).

Tree detection

Individual trees were delineated for ten years (2000, 2003, 2005, 2007–2011, 2013 and 2015) based on aerial images which were captured and georeferenced by Georeal. The aerial imagery has a 20 cm spatial resolution. ArcGIS (Esri 2013) was used for spatial data processing and SAGA GIS (Conrad et al. 2015) was used mostly for DEM analysis. An individual tree point layer was first created for 2000. Each tree in the vectorised point layer was manually classified to one of 6 categories based on visual interpretation: adult healthy, adult dead, young healthy, young dead, stump, or sapling (see Table 1). To minimise errors during vectorisation, in every following aerial photograph, every single tree presence was validated as a new attribute in the table, reflecting its health condition in a particular year.

Tree conditions were assessed mainly by changes in crown colour; a **healthy** tree (not affected tree) in aerial photos appears in many shades of green, while **dead** (or dying) trees (affected trees) appear as orange, brown, grey or white (grey attack); category **stump** was used for the remaining stumps when trees fell down (standing stumps). Categories **adult** and **young** were classified according to crown projection, (see Fig. 1) combined with visual interpretation of the aerial images (difference in crown shape and diameter). The terrain slope and elevation were also considered. The category **sapling** covers newly appearing trees. When the crown diameter exceeded 2 m it was moved to category **young healthy** tree.

Each tree in the basin and most of the trees in the buffer zone (where a digital elevation model was available) has an attribute of its topography (altitude, aspect, slope, and sub-basin delineation) which was calculated from the digital elevation model (spatial resolution 0.2 m).

Tree height

The categories **young** and **adult** correspond with tree height (7–20 m, 20–50 m), respectively. The height was added to each tree later after analysing heights from the LiDAR points.

The ground-based LiDAR data (points with elevation value) acquired from 2008 and 2011 were combined in one dataset and transformed to the grid (pixel size 20 cm, pixel value corresponds to the local maximum of the points within a given pixel). LiDAR point clouds

Table 1. Amount of tree categories present in the basin in the observed time segments according to their health and height conditions.

Category/Year	2000	2003	2005	2007	2008	2009	2010	2011	2013	2015
Adult healthy	16148	14841	11025	6089	4851	2513	2383	2133	2103	2065
Adult dead	1178	2436	5600	8724	8793	9890	8732	7293	3863	1688
Young healthy	3227	3217	3129	2952	2845	2722	2766	3698	4375	5596
Young dead	14	24	109	262	314	441	385	437	352	141
Stump	13	62	717	2560	3786	5050	6413	8151	11699	14198
Sapling	774	1180	2631	3596	4282	4938	6981	9275	18237	37646
Total (No. of saplings)	**20580**	**20580**	**20580**	**20587**	**20589**	**20616**	**20679**	**21712**	**22392**	**23688**
Total	**21354**	**21760**	**23211**	**24183**	**24871**	**25554**	**27660**	**30987**	**40629**	**61334**

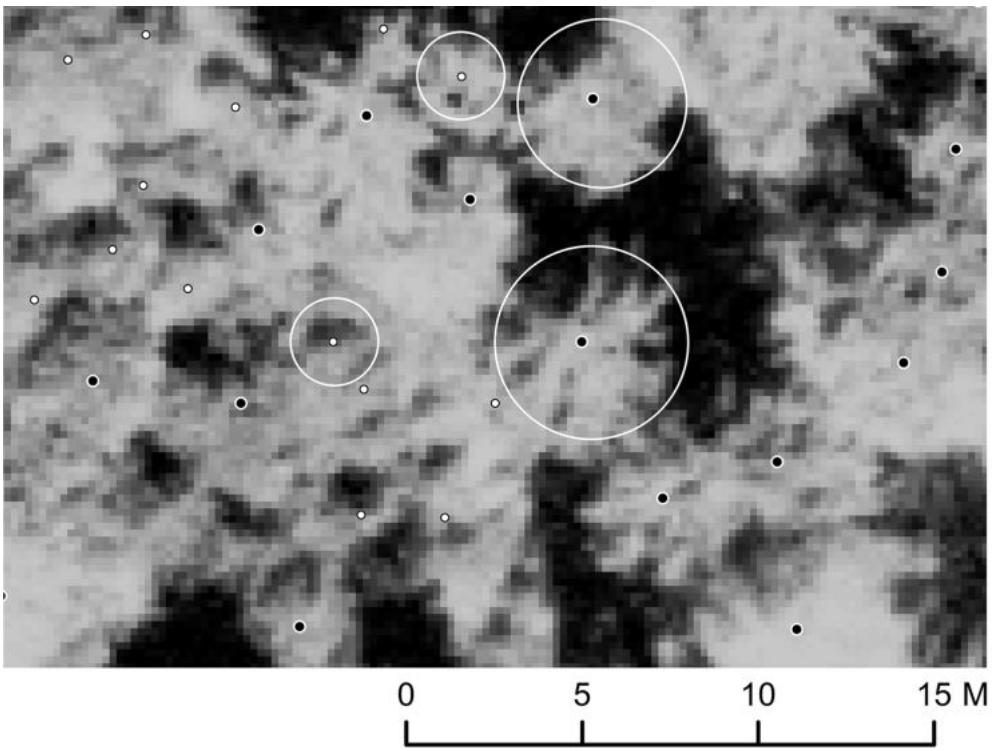

Fig. 1. Definition of young and adult tree categories based on crown projection. Black points represent adults and white points represent young trees. White circles show a sample of crown projection. This figure shows only the relative differences in diameter of the crown projection as one parameter for distinction between young and adult trees.

for different years (2008, 2011) covered different parts of the area. The difference in tree growth between the two years was neglected. The height of every single tree, except category **sapling**, was assigned to the tree stands in a geodatabase (**layer tree stands**) in two steps.

Circular crown projections for each individual surviving tree were manually (quality of the data does not allow automatic detection) derived from the local maximum grid. We combined LiDAR data with a visual interpretation of the aerial photographs to attain the highest accuracy of individual tree delineation. Centroids of the crown projections were then converted to the point layer (**layer tree height**) with local maximum height values. First, we found trees in the layer tree height which matched the closest trees in the layer tree stand **healthy young** and **dead young** tree values between 7 and 25 m. This way we matched 11 711 tree heights. We separated young (2 419 individuals) and adult (9 292 individuals) trees and for both subsets interpolated individual natural neighbour rasters (**adult** tree raster, **young** tree raster) with 10 m spatial resolution and filtered to derive a mean height value per hectare afterwards. This step ensures the variability in tree heights and reflects the site stand characteristics. Height values for all trees which were not assigned with the layer tree height before (gaps in LiDAR data) were assign an interpolated pixel value from these newly created rasters (high trees and stumps from the **adult tree raster**, young trees from the **young tree raster**).

Tree height was not calculated for all trees in the buffer zone since LiDAR was not available for the entire area so it was not possible to create a natural neighbour raster covering all the buffer area. Moreover, in 2007, 255 trees were clear-cut in the upper part of the basin which belongs to Austria. It was not possible to create a natural neighbour raster for those trees; therefore we used the average height of 20.5 m, estimated from approximately 700 trees in the close surrounding (up to 60 m). We excluded all broadleaf trees (693 individuals from the basin and 462 individuals from the buffer zone) and also (due to technical limitations of the Simp D model by Wirth et. al. 2004) trees below 7 m in height.

We assigned 23 485 heights of coniferous trees altogether in the first and second steps (from which 15% of trees are in the buffer zone). Based on matching coordinates, we validated the tree heights extracted from the tree height rasters using data measured in the field during previous studies (Svoboda et al. 2006b, Matějka 2009). Due to the low number of surviving trees in the year of LiDAR scanning we were able to match only 90 individuals. The trees in our study were 0.46 m (SD = 3.67) lower than those in the above-mentioned studies.

Tree DBH

The current approach is to derive DBH as one of the tree characteristics from the LiDAR scan of the trees using various techniques like multiple scan (Korpela et al. 2010), full-waveform LiDAR data (Yao et al. 2012) or random forest segmentation (Yu et al. 2011). This was not done in our case due to missing more LiDAR data (difficulty with LiDAR scanning in coarse terrain). To estimate the DBH for every tree, we used equation (1), which is based on real data measurements (approximately 1500 samples from elevations within 700–1400 m a.s.l.) from surrounding areas close to the study area (Cienciala – unpubl.). This relationship between tree height and DBH for tree samples within a specific elevation value corresponds to our study area (see Fig. 2).

$$DBH = A \times tree\ height^{B} \times \left(\frac{elevation}{1000} \right)^{C} \qquad R^2 = 0.83 \tag{1}$$

The coefficients (A, B, C) for DBH dependency on the tree height are shown in Table 2.

Tree biomass estimation

We divided biomass into different components in order to quantify such parts (roots, stem, bark, branches, needles) for different purposes and utilization (KÖHL et al. 2006). With respect to the fact that the choice of a biomass estimation model is mostly the main source of uncertainty and errors in forest biomass calculations (SILESHI 2014), it is important to look at a species specific model.

For individual trees, we calculated the dry weight in kg of a particular tree compartment (needles, branches, dry branches, stem and roots) according to WIRTH et al. (2004) using Simp D models. With the aim to compare results with data shown in SVOBODA et al. (2006b), we divided stem to bark and wooden part by following equations:

Stem wood $y = (2.4298 \ln(x) + 84.042) \times s \quad R^2 = 0.55$ (2)

Stem bark $y = (-2.43 \ln(x) + 15.958) \times s \quad R^2 = 0.5$ (3)

Where x is tree height in m and s is biomass of stems in kg and dry and living branches were merged together (all branches) and later divided (different compartments according to SVOBODA et al. (2006) to categories: branch wood, branch bark and fine branches by the following equations:

Branch wood $y = (15.512 \ln(x) + 11.516) \times b \quad R^2 = 0.49$ (4)

Branch bark $y = (0.8226 \ln(x) + 16.379) \times b \quad R^2 = 0.03$ (5)

Fine branches $y = (-16.34 \ln(x) + 72.105) \times b \quad R^2 = 0.42$ (6)

Where x is tree height in m and b is the biomass of all branches in kg.

Approximately 255 trees, clear-cut in 2007 in Austria, were partially excluded from the calculations. Aboveground tree biomass from this area was harvested; therefore only underground biomass of these trees is counted in the biomass estimation. Spatial distribution of the biomass volume recalculated from the number of trees is shown in a raster format with pixel size of 20 m. The pixel values for biomass estimation represent the biomass volume within 1 ha. Firstly, we created a regular net of the cells to cover the whole basin area (same spatial extent as DEM) and derived central points for every cell. Then a circular polygon (buffer around the point) with area equal to 1 hectare was made for each cell. The biomass volume for a given category (total, live trees, dead trees) was finally summarized for all trees lying including the catchment's buffer area. Therefore, volume per hectare respects the tree volume exactly counted within the area. It is important to emphasize that, although biomass estimation corresponds with the number of vectorized trees, the volume accuracy is still affected by errors during vectorization trees and estimation errors, which comes from the whole-tree biomass allocation patterns and allometric functions (WIRTH et al. 2004). We used

Table 2. Estimated parameters for DBH equation calculation. A, B, C are regression parameters in equation (1) respectively. ASE means asymptotic standard error for regression model.

Parameter	Estimate	ASE	Parameter/ASE	Wald 95% Confidence Interval	
				Lower	Upper
A	0.682	0.019	36.217	0.645	0.718
B	1.240	0.008	149.752	1.224	1.256
C	1.051	0.018	57.568	1.015	1.087

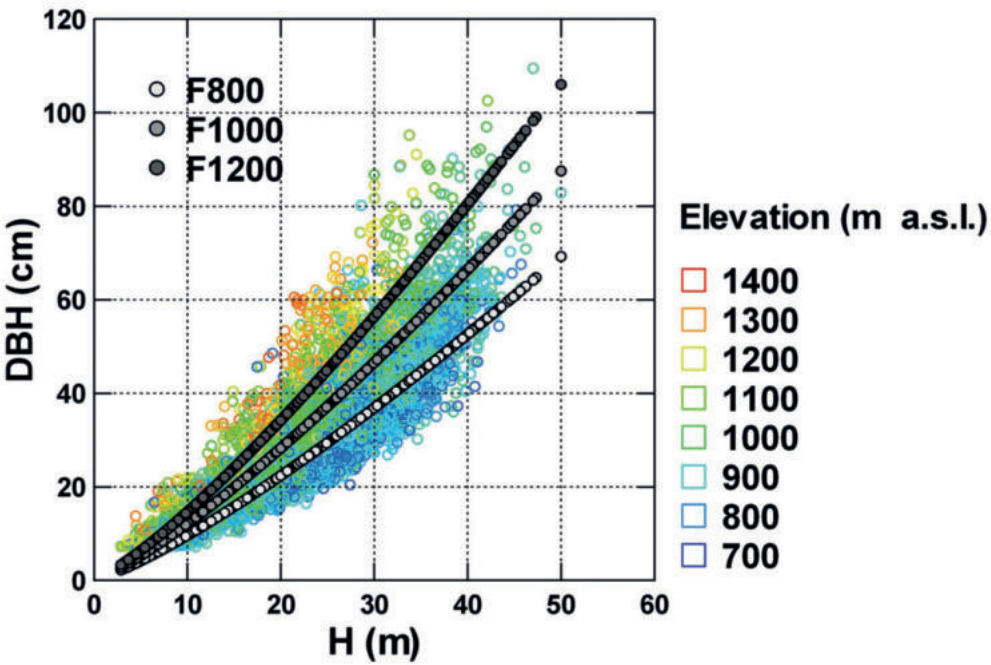

Fig. 2. Model of dependence of DBH on tree height according to elevation for equation (1) (Cienciala unpubl.). Modelled values for elevations (F) 800, 1000 and 1200 m a.s.l., are highlighted.

the same method to create a raster for the number of trees per hectare in 2011 and the number of saplings per hectare in 2013.

Spruce biomass was calculated as a combination of the number of trees present in the basin in 2011 (including dead lying wood) and tree heights from the LiDAR data of 2008 and 2011. Therefore, it represents the total tree biomass in 2011, which was calculated as if they were living (standing) trees (details of tree category proportions in Table 1). For two reasons, only trees with a diameter of at least 7 cm were used. Firstly, we assumed that trees with a 7 cm diameter or above were already present in the basin in 2000, secondly, the biomass estimation method used to calculate biomass (Wirth et al. 2004) is not suitable for trees under 7 cm in DBH. The final summarization of the biomass is expressed in volume per spatial area unit, i.e. tons of dry weights per hectare (t/ha).

Results

Altogether, there were originally 21 354 trees in the basin in 2000, of which 19 375 trees were living, 1205 were dead or dying and 774 were recognized as saplings (Table 1). The density distribution of the adult trees since 2000 is shown in Fig. 3. Since 2000, the amount of dead trees doubled every 2 years, and this trend continued till 2007 (1317 new cases in 2003, 3904 new cases in 2005 and 5120 new cases in 2007). Since 2007, the process of infecting new individuals decreased (3835 new cases between 2007 and 2009) to the minimum (646 new cases between 2009 and 2015).

When comparing the tree numbers according to height between 2000 and 2015, the main losses were with trees taller than 15 m while the change of tree numbers below this height was negligible (Fig. 4). A massive growth of young trees since 2009 can be seen in the aerial photographs. In addition, approximately 1800 trees moved to a higher level category (saplings into young healthy trees or young healthy trees into adult healthy trees). The dynamic of the forest decline is shown in Fig. 5. The break point between forest decline and forest regeneration can be seen around 2009 with natural forest regeneration being faster after that year. There was a 60.5% loss of standing trees in the basin when comparing the amount of trees in 2000 and 2015 (see Fig. 6). The spatial distribution of surviving trees in 2015 can be seen in Fig. 6C. In comparison with the percentage of dead trees, the total amount of standing trees is replaced by an increasing number of saplings. The distribution of saplings per hectare corresponds to the areas with a high density of dead or dying trees over time (Fig. 7A). The locations with higher numbers of saplings after infestation (2015) are located on the western and eastern parts of the basin (Fig. 7A).

In 2000, the dead trees (5.85% of total tree amount) were randomly and sparsely distributed over the entire area (see Fig. 6A). The first decline of trees in 2003 appeared in the upper and flat part and low plain in the centre of the basin (see Fig. 3A). The amount of infected trees doubled within these three years (6.4% newly dead trees of the total). Infected trees spread to nearby neighbouring trees in the north part of the basin. Later, between 2003 and 2005, newly infected trees appeared densely in the entire basin (19.0% new cases of the total amount, see Fig. 3B). The most intensive decline of trees (24.9% newly dead trees of the total amount) occurred between 2005 and 2007. The most affected part was in the eastern basin part (Fig. 3C). Massive declines can also be seen in the highest parts (above 1300 a.s.l.) at the basin corner from the west-south, south and east-south border. During 2007–2008, the speed

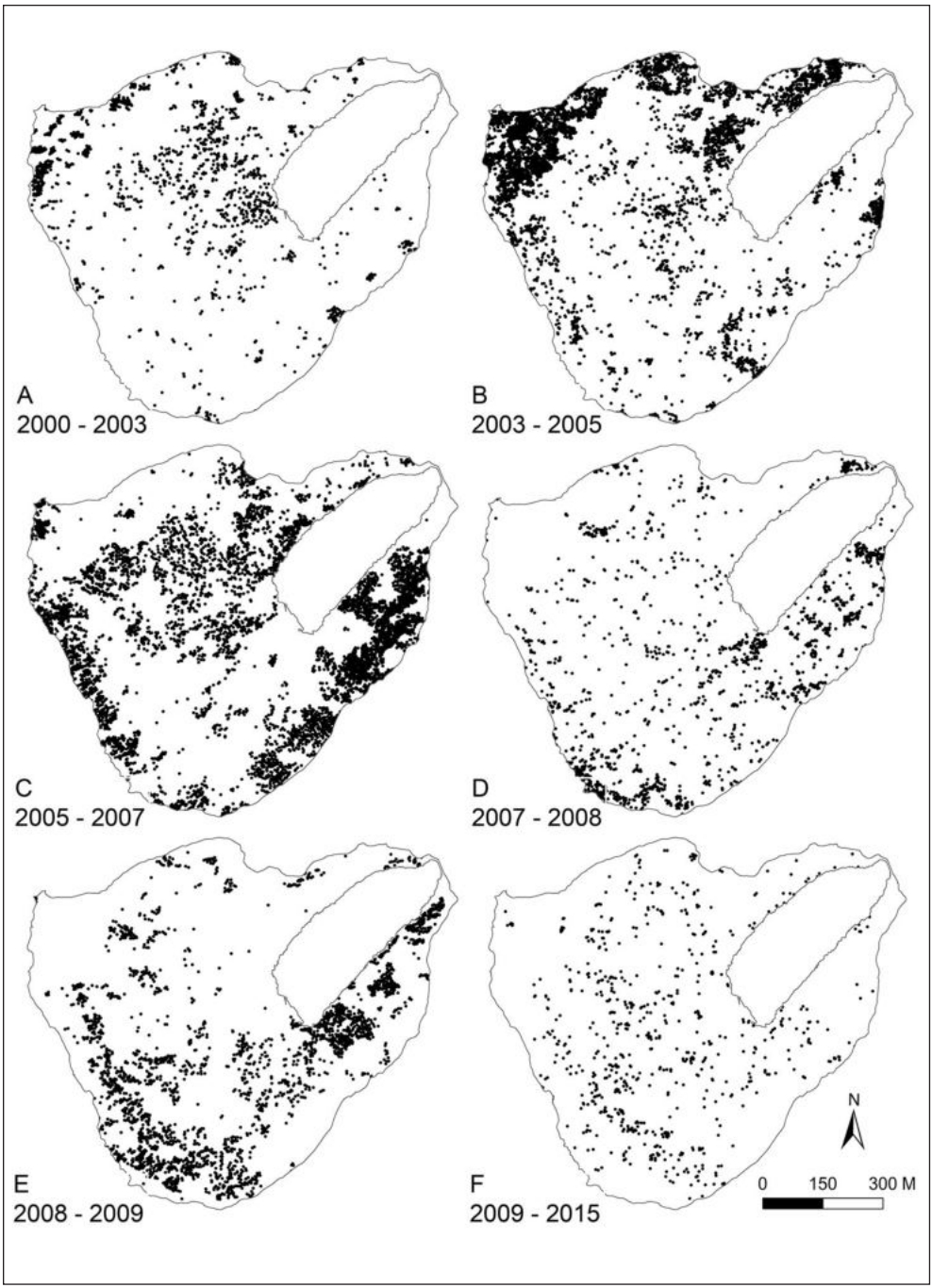

Fig. 3. Detailed position of newly appearing dead or dying trees within particular periods.

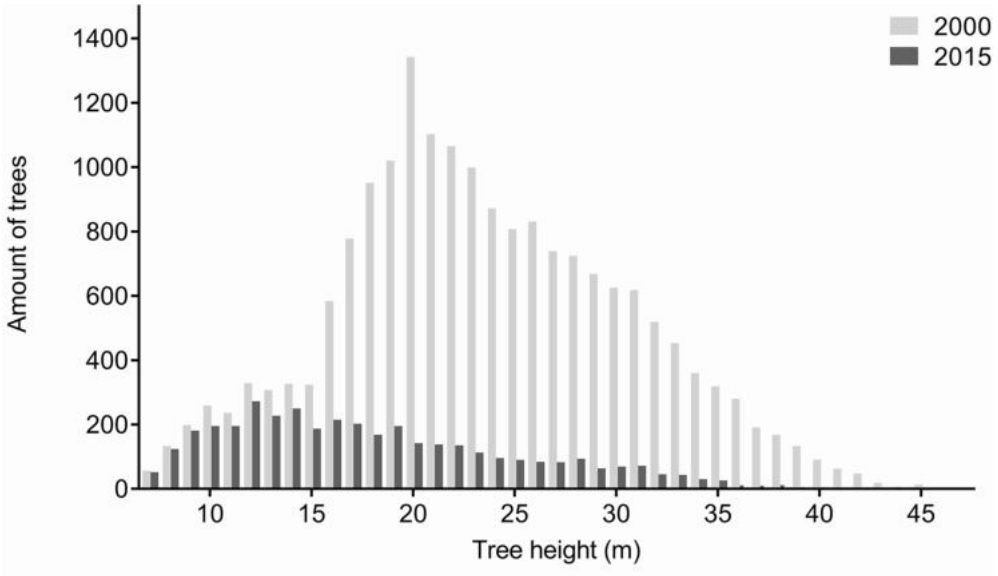

Fig. 4. Histogram for living tree amount according to tree height within the basin. Light grey colour represents the original amount of trees in 2000 and dark grey represents trees surviving till 2015.

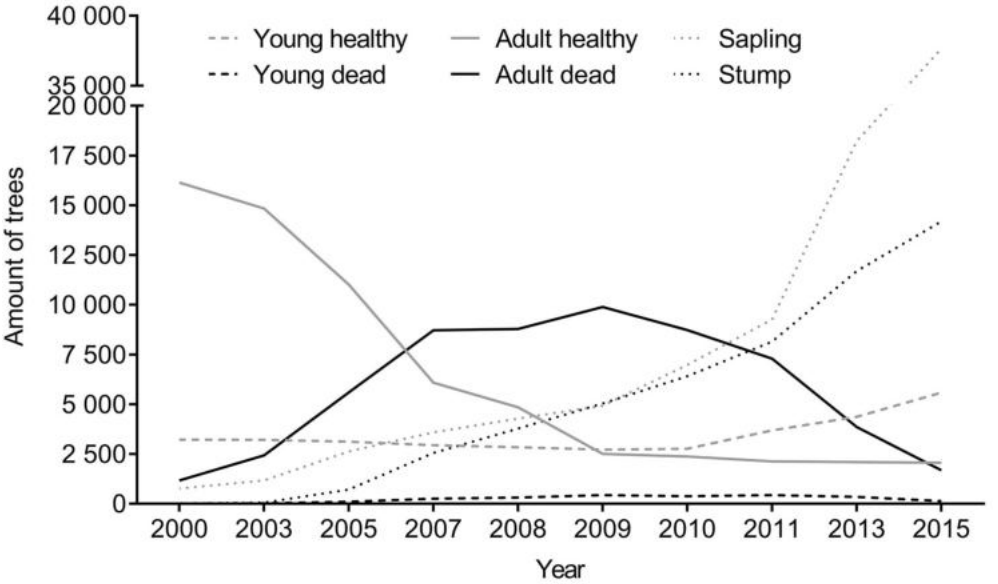

Fig. 5. The progress of tree condition during the period 2000–2015, the amount of total trees and trees in 6 categories and the development of tree death and sapling growth in 10 particular years along the forest decline process.

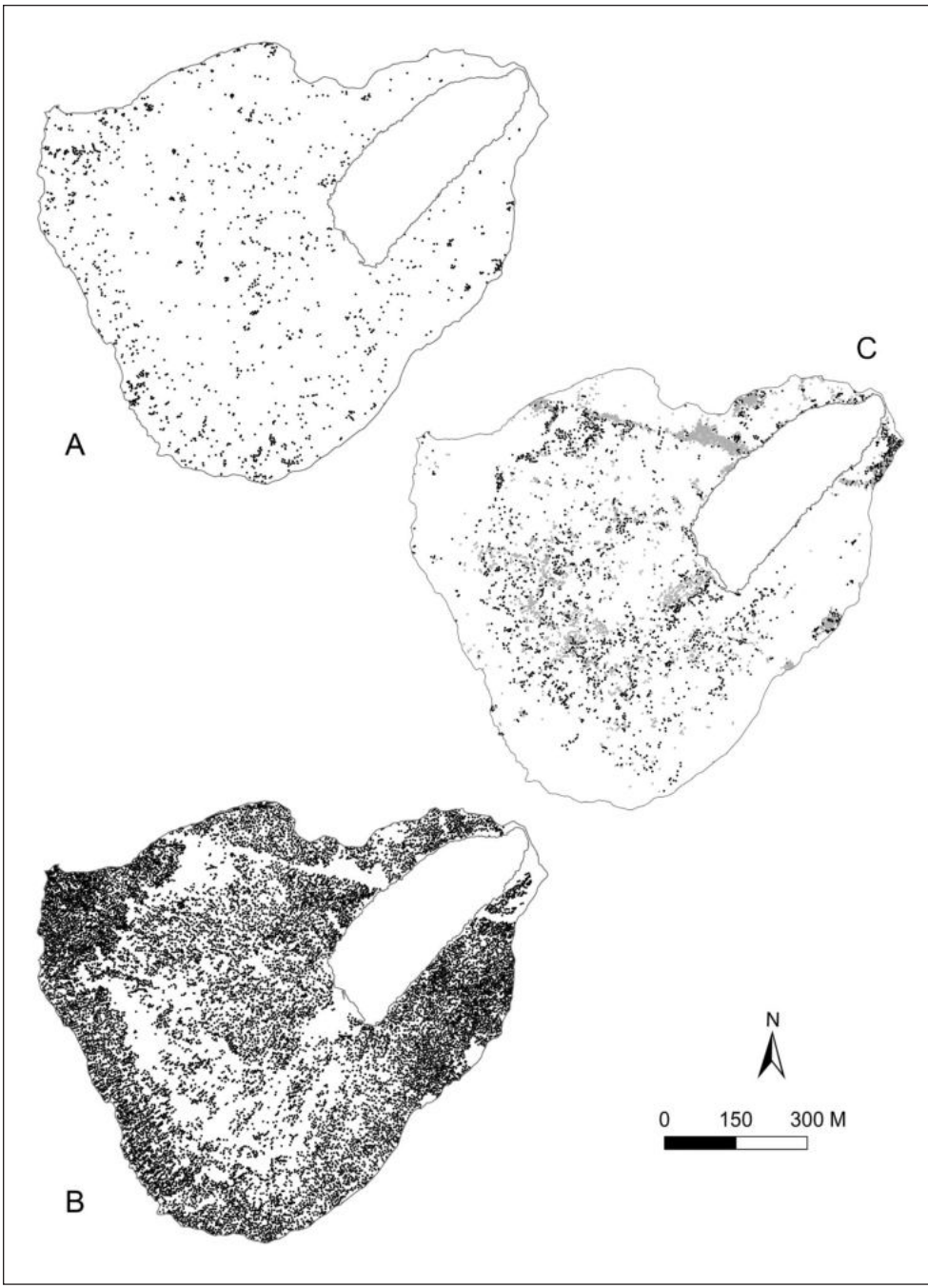

Fig. 6. Detailed position of all dead or dying trees in years: A – 2000, B – 2015 and all surviving trees in 2015 (black point – adult trees, grey point – young trees) – C.

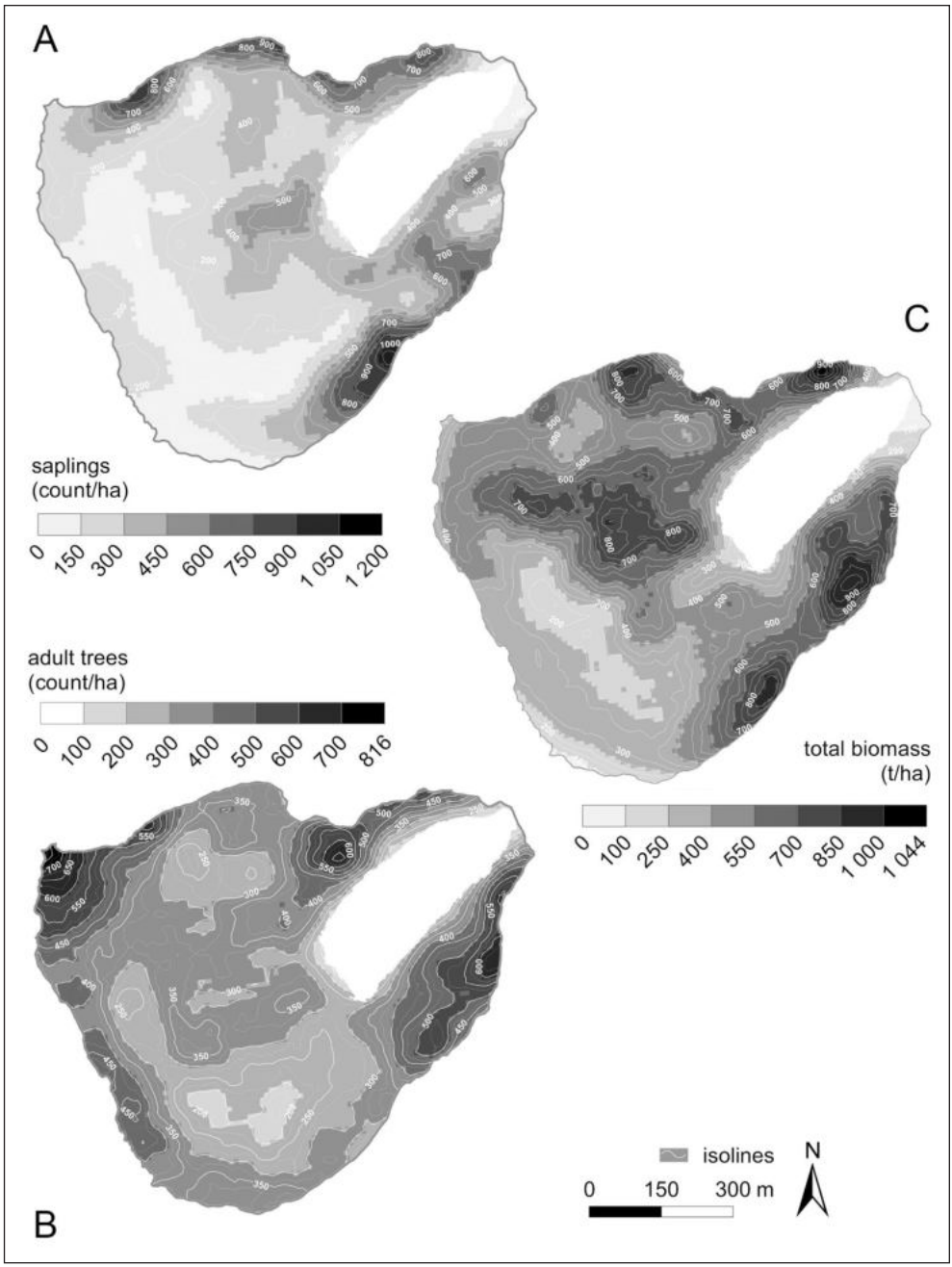

Fig. 7. Amount of adult trees (including dead individuals and stumps) per hectare in 2000 (A), amount of saplings per hectare in 2013 (B) and total biomass distribution: adult tree-, young tree- and stump biomass in tons per hectare in 2011.

of stand decline decreased (6.5% of new cases) and newly attacked trees were distributed more randomly (Fig. 3D), while in 2008–2009 a massive spreading (12.1% new cases of total) appeared in the upper southern basin part and lower eastern part (Fig. 3E). Since 2009, just a few trees in the whole area died compared to previous years (3.1% of new cases till the summer 2015, Fig. 3F). In 2015, the total amount of dead trees reached 77.9% of the original amount (20 580 individuals, Fig. 6B) in 2000.

Biomass

The total estimate of tree biomass in the Plešné Lake basin was 28 329 tons of dry biomass. From that, 1 148 tons were needles, 2 440 tons branches, 17 960 tons stem and 6 781 tons roots. Average biomass was 504.4 t/ha ranging from 345.1 t/ha to 672.9 t/ha. Biomass per area corresponds with the average slope (see Fig. 7C). The places with higher values of estimated volume were located at the north and south borders of the basin (high density biomass volume patches) and in the central part of the Plešné cirque. The lowest values of biomass were centred on the steepest parts of the cirque and very close to the lake (Fig. 7C).

Discussion

Forest decline in our study area occurred from 2007–2009, when there was the highest number of trees affected. This corresponds with high bark beetle densities, which affected Norway spruce stands also in other localities in the Šumava Mountains (e.g. Hais et al. 2009). The estimation of forest volume biomass documents the high level of wood storage in the basin of Plešné Lake. Combining both these results contributes to understanding forest disturbance dynamics in connection with the use of dead wood biomass for decomposition following forest recovery.

Dynamic of forest decline due to bark beetle

Insect forest disturbance results in a typical mosaic of living and dead trees. This is made by way of spruce bark beetle dispersion, which forms a mosaic of 5–10 dead trees patches in a living forest at the beginning of the outbreak (Wermelinger 2004). In our study, we identified the first patches of dead trees in 2003 followed by a massive infestation in 2004. However, the spreading of bark beetle was not continuous. Similarly to results of Berec et al. (2013), we consider climate as the strongest influence on bark beetle spreading. Climate may influence bark beetle mortality, due to negative temperature extremes during the winter, while on the other hand warm and dry summers support the maturation of bark beetle larvae. Simultaneously, such weather conditions may increase spruce water stress and thus tree susceptibility to bark beetle affectation. This may explain the increase in bark beetle forest infestation during the years following warmer winters (2006–2007) or a warmer spring (2008) and warmer summers (2003, 2011 and 2012) (Fig. 8). This result documents the general relation between bark beetle infestation and climate and/or meteorological factors, since the northern aspect of the Plešné Lake basin reduces the influence of incident solar radiation on the SW slopes, which is reported as a critical factor for bark beetle infestation (e.g. Berec et al. 2013). However, as soon as the bark beetle reached some threshold of population density,

which is needed to overwhelm tree defences, the bark beetle became less selective together with a lower importance of environmental factors (Lausch et al. 2011).

In fact the strongest bark beetle forest infestation occurred prior to 2009 when 14 176 trees (68.8%) died in the basin. Since that time, only a few trees per year died compared to those previous years (3.1% last six years of study). Despite the high mortality of adult trees, the mortality of young trees up to 15 m height was negligible. This corresponds with bark beetle preference to attack trees older than 60 years (e.g. Wermelinger B. 2004). Surviving trees remain mostly in shaded locations with steep slopes inside the basin cirque. One of the reasons for tree survival in those localities is the balanced water regime of the shaded areas, which should be less affected by summer water stress. Another positive feature of terrain ruggedness for tree survival is the high local variation in environmental conditions, which can cause stand fragmentation (Senf & Seidl 2018). The regenerating forest following the insect disturbance contains the remaining surviving adult trees which are important as seed sources. The seedlings, together with young trees, increase their growth rate because they are no longer limited by light after canopy defoliation. On the contrary, clear-cutting forest management results in higher disturbance severity due to removal of the entire canopy including seedlings and saplings (Hais et al. 2009).

Despite that the estimate of newly appearing trees (saplings) numbers is a rough guess due to detection limitations from aerial photographs, there is an obvious two level increase in their amount (2005, 2011). We suppose this relates to defoliation and forest decline, which results in increased incoming solar radiation needed to grow the young trees. On the contrary, the estimate of young trees was limited by canopy closure, which means that these young trees were underestimated before canopy defoliation. However, this result still provides valuable information as there was no field study within the basin till 2005 (see Svoboda et al. 2006a,b). A field study would be more appropriate in providing an accurate number of trees.

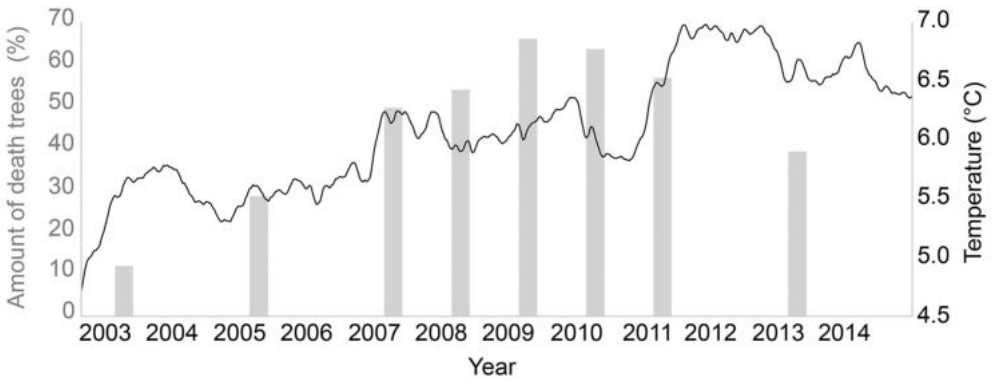

Fig. 8. Trend (moving average for a 30 day period) in daily temperature amplitudes measured 2 m above ground (Turek 2014) in the higher part of the basin (in all other research papers referred as study site PL2 e.g. (Kopáček et al. 2002). Peaks in 2003, winter 2007/2008 and 2011 are related to warmer weather, but slow amplitude increase in temperature oscillations during the entire period can still be recognized. The related amount of dead trees for the appropriate year is shown in grey colour.

Biomass

Norway spruce biomass production is determined by many environmental variables such as a soil, water and nutrients, incoming solar radiation, topography and tree competition. The resulting tree biomass plays a crucial role in the disturbance regime and represents an important nutrient pool which can be used for forest regeneration after forest decay.

Compared to Svoboda et al. (2006a,b), we found a different amount of root biomass. Our root biomass estimation is 22.2% of total tree biomass. Both estimation values (our results and Svoboda et. al 2006) for root biomass are approximately the same up to a DBH of around 40 cm for trees with similar height, DBH and aboveground distribution. With greater DBH and tree heights, the root biomass estimation shows higher variability (10% to 50% for the different DBH categories considered in Svoboda et al. 2006a), which means that our total single tree biomass varies 1–16%. The accuracy of the biomass estimation may be influenced by the quality of the relation between the DBH and partial biomass. Despite of the limited number trees used for these relationships (Svoboda et al. 2006b), the fit quality for stem biomass is quite high ($R^2 = 0.55$). On the contrary, the quality of fit for the branch wood categories relating to DBH is much lower, where the highest uncertainty is in the case of branch bark ($R^2 = 0.03$). However, branch bark has the lowest relation to the entire tree biomass.

The final estimation of total biomass in the Plešné Lake basin was 504.4 t/ha. Our aboveground biomass estimation (403.9 t/ha) corresponds with the results of the Czech Terra project (Cienciala et al. 2015), where the estimated above ground Norway spruce biomass was 414 t/ha for the age class 121–140 years. Previous models published by Svoboda et al. (2006b) for the Plešné Lake basin (133.58 t/ha) and Matějka (2009) (197 t/ha) seem to underestimate biomass, even though Svoboda et al. (2006a,b) used the same allometric equations by Wirth et al. (2004) as in our study. We suppose that one of the reasons for the difference is that these authors neglected the younger trees (minimal DBH used in Svoboda (2006a,b) 28 cm and 24 cm in Matějka (2009) compared to our 8.4 cm). But more probably it shows that semiautomatic methods based on tree detection from aerial photographs in such a complicated terrain are not sufficient and a different approach is necessary.

Conclusion

Our study describes the dynamics of Norway spruce forest decline during a bark beetle infestation and its natural recovery in the Plešné Lake basin (the Šumava Mountains). The highest number of affected adult trees occurred in 2009 (74.6% of trees in basin were dead), which was probably caused by the highest bark beetle densities. However, there are other peaks during the forest decline, which may be related to warmer years supporting bark beetle maturation and spreading. The defoliation of adult tree canopy accelerated the growth of young trees and saplings, which were limited by a lack of light.

The Norway spruce total biomass estimation in the Plešné Lake basin was 504.4 t/ha on average, which is a higher value than found in previous models, however, this value corresponds to the results of recent studies in old-growth forests or for older age classes.

The presented results can help us understand the processes during the infestation and natural decline of mountain spruce forest, and also to estimate the development of bark beetle infestation and natural forest recovery in similar areas surrounding other glacial lakes in the Šumava Mountains.

Acknowledgement. We thank K. Matějka and E. Cienciala for reference data and the tree heights/DBH model. We are grateful to K. Edwards for language improvements. This study was supported by the Grant Agency of the Czech Republic (project No. P503/19/16605S).

References

Aerts R. & Honnay O., 2011: Forest restoration, biodiversity and ecosystem functioning. *BMC Ecology*, 11: 29.

Berec L., Doležal P. & Hais M., 2013: Population dynamics of *Ips typographus* in the Bohemian Forest (Czech Republic): Validation of the phenology model PHENIPS and impacts of climate change. *Forest Ecology and Management*, 292: 1–9.

Bengtsson J., Nilsson S.G., Franc A. & Menozzi P., 2000: Biodiversity, disturbances, ecosystem function and management of European forests. *Forest Ecology and Management*, 132: 39–50.

Cienciala E., Černý M., Russ R. & Zatloukal V., 2015: Inventarizace krajiny CzechTerra. Vybrané výsledky šetření z let 2008/2009 a 2014/2015. *Lesnická práce*, 10.

Cohen W.B., Spies T.A. & Fiorella M., 1995: Estimating the age and structure of forests in a multi--ownership landscape of western Oregon, U.S.A. *International Journal of Remote Sensing*, 16: 721–746.

Conrad O., Bechtel B., Bock M., Dietrich H., Fischer E., Gerlitz L., Wehberg J., Wichmann V. & Böhner J., 2015: System for Automated Geoscientific Analyses (SAGA) v. 2.1.4. *Geoscientific Model Development*, 8: 1991–2007.

ESRI (Environmental Systems Research Institute), 2013: ArcGIS Desktop 10.2.

Frelich L., 2016: Forest dynamics. F1000Research. 5. 10.12688/f1000research.7412.1.

Frelich L.E., Jõgiste K., Stanturf J.A., Parro K. & Baders E., 2018: Natural Disturbances and Forest Management: Interacting Patterns on the Landscape. In: *Ecosystem Services from Forest Landscapes*, Perera A., Peterson U., Pastur G., Iverson L. (eds) Springer, Cham: 221–248.

Geiger R., Aron R.H. & Todhunter P., 2003: *The climate near the ground*. Sixth edition. Rowman & Littlefield Publishers, Inc., Langham etc., 584 pp.

Gregoire T.G. & Valentine H.T., 2007: *Sampling Strategies for Natural Resources and the Environment*. CRC Press, 494 pp.

Hais M. & Kučera T., 2008: Surface temperature change of spruce forest as a result of bark beetle attack: Remote sensing and GIS approach. *European Journal of forest research*, 127: 327–336.

Hais M., Jonášová M., Langhammer J. & Kučera T., 2009: Comparison of two types of forest disturbance using multitemporal Landsat TM/ETM+ imagery and field vegetation data. *Remote Sensing of Environment*, 113: 835–845.

Hais M., Wild J., Berec L., Brůna J., Kennedy R., Braaten J. & Brož Z., 2016: Landsat Imagery Spectral Trajectories–Important Variables for Spatially Predicting the Risks of Bark Beetle Disturbance, *Remote Sensing*, 8: 687.

Hauglin M., Dibdiakova J., Gobakken T. & Næsset E., 2013: Estimating single-tree branch biomass of Norway spruce by airborne laser scanning. *ISPRS Journal of Photogrammetry and Remote Sensing*, 79: 147–156.

Jean M., Lafleur B., Fenton N., Paré D. & Bergeron Y., 2019: Influence of fire and harvest severity on understory plant communities. *Forest Ecology and Management*, 436: 88–104.

Jonášová M. & Prach K., 2004: Central-European mountain spruce (*Picea abies* (L.) Karst.) forests: regeneration of tree species after a bark beetle outbreak. *Ecological Engineering*, 23: 15–27.

Kangas A. & Maltamo M., 2009: *Forest Inventory: Methodology and Applications*. Springer, 362 pp.

Kankare V., Holopainen M., Vastaranta M., Puttonen E., YU X., Hyyppä J., Vaaja M., Hyyppä H. & Alho P., 2013: Individual tree biomass estimation using terrestrial laser scanning. *ISPRS Journal of Photogrammetry and Remote Sensing*, 75: 64–75.

Köhl M., Magnussen S. & Marchetti M., 2006: *Sampling Methods, Remote Sensing and GIS Multiresource Forest Inventory (Tropical Forestry)*. Springer, 373 pp.

Kopáček J., Kaňa J., Šantrůčková H., Porcal P., Hejzlar J., Picek T. & Veselý J., 2002: Physical, chemical and biological characteristics of soils in watersheds of the Bohemian Forest lakes: I. Plešne Lake. *Silva Gabreta*, 8: 43–66.

Kopáček J., Cosby B.J., Evans C.D., Hruška J., Moldan F., Oulehle F., Šantrůčková H., Tahovská K. & Wright R.F., 2013: Nitrogen, organic carbon and sulphur cycling in terrestrial ecosystems: linking nitrogen saturation to carbon limitation of soil microbial processes. *Biogeochemistry*, 115: 33–51.

Kopáček J., Bače R., Hejzlar J., Kaňa J., Kučera T., Matějka K., Porcal P. & Turek J., 2020: Changes in microclimate and hydrology in an unmanaged mountain forest catchment after insect-induced tree dieback. *Science of the Total Environment*, 720: 137518.

Korpela I., Ole Ørka H., Maltamo M., Tokola T. & Hyyppä J., 2010: Tree species classification using airborne LiDAR – effects of stand and tree parameters, downsizing of training set, intensity normalization, and sensor type. *Silva Fennica*, 44: 319–339.

Krankina O.N., Harmon M.E. & Griazkin A.V., 1999: Nutrient stores and dynamics of woody detritus in a boreal forest: modeling potential implications at the stand level. *Canadian Journal of Forest Research*, 29: 20–32.

Lausch A., Fahse L. & Heurich M., 2011: Factors affecting the spatio-temporal dispersion of *Ips typographus* (L.) in Bavarian Forest National Park: A long-term quantitative landscape-level analysis. *Forest Ecology and Management*, 261: 233–245.

Lausch A., Heurich M. & Fahse L., 2013: Spatio-temporal infestation patterns of *Ips typographus* (L.) in the Bavarian Forest National Park, Germany. *Ecological Indicators*, 31: 73–81.

Matějka K., 2009: Assessment of tree layer biomass and structure using aerial photos in lake catchments of the Šumava Mts. *Journal of Forest Science*, 55: 63–74.

Morsdorf F., Meier E., Kötz B., Itten K.I., Dobbertin M. & Allgöwer B., 2004: LIDAR-based geometric reconstruction of boreal type forest stands at single tree level for forest and wildland fire management. *Remote Sensing of Environment*, 92: 353–362.

Netherer S. & Nopp-Mayr U., 2005: Predisposition assessment systems (PAS) as supportive tools in forest management—rating of site and stand-related hazards of bark beetle infestation in the High Tatra Mountains as an example for system application and verification. *Forest Ecology and Management*, 207: 99–107.

Neuhäuslová Z., 2001: The Map of Potential Natural Vegetation of the Šumava National Park. Explanatory text, *Silva Gabreta*, Suppl. 1.

Newton A., 2007: *Forest Ecology and Conservation: A Handbook of Techniques*. Oxford University Press, 454 pp.

Parresol B.R., 1999: Assessing tree and stand biomass: A review with examples and critical comparisons. *Forest Science*, 45: 573–593.

Pickett S.T.A., 1986: *The Ecology of Natural Disturbance and Patch Dynamics*. Academic Press, 472 pp.

Repola J., 2009: Biomass equations for Scots pine and Norway spruce in Finland. *Silva Fennica*, 43: 625–647.

Rozman A., Diaci J., Krese A., Fidej G. & Rozenbergar D., 2015: Forest regeneration dynamics following bark beetle outbreak in Norway spruce stands: Influence of meso-relief, forest edge distance and deer browsing. *Forest Ecology and Management*, 353: 196–207.

Senf C. & Seidl R., 2018: Natural disturbances are spatially diverse but temporally synchronized across temperate forest landscapes in Europe. *Global change biology*, 24(3): 1201–1211.

Sileshi G.W., 2014: A critical review of forest biomass estimation models, common mistakes and corrective measures. *Forest Ecology and Management*, 329: 237–254.

Svoboda M., Matějka K. & Kopáček J., 2006a: Biomass and element pools of understory vegetation in the catchments of Čertovo Lake and Plešné Lake in the Bohemian Forest. *Biologia*, 61: S509–S521.

Svoboda M., Matějka K., Kopáček J. & Žaloudík J., 2006b: Estimation of tree biomass of Norway spruce forest in the Plešné Lake catchment, the Bohemian Forest. *Biologia*, 61: S523–S532.

Svoboda M., Fraver S., Janda P., Bače R. & Zenáhlíková J., 2010: Natural development and regeneration of a Central European montane spruce forest. *Forest Ecology and Management*, 260: 707–714.

Vepakomma U., St-Onge B. & Kneeshaw D., 2008: Spatially explicit characterization of boreal forest gap dynamics using multi-temporal lidar data. *Remote Sensing of Environment*, 112: 2326–2340.

Wang L., Gong P. & Biging G.S., 2004: Individual Tree-Crown Delineation and Treetop Detection in High-Spatial-Resolution Aerial Imagery. *Photogrammetric Engineering & Remote Sensing*, 70: 351–357.

Wermelinger B., 2004: Ecology and management of the spruce bark beetle Ips typographus – a review of recent research. *Forest Ecology and Management*, 202: 67–82.

Wirth C., Schumacher J. & Schulze E.-D., 2004: Generic biomass functions for Norway spruce in Central Europe – a meta-analysis approach toward prediction and uncertainty estimation. *Tree Physiology*, 24: 121–139.

Wulder M.A. & Franklin S.E., 2006: *Understanding Forest Disturbance and Spatial Pattern: Remote Sensing and GIS Approaches*. CRC Press, 246 pp.

Wulder M.A., White J.C., Nelson R.F., Næsset E., Ørka H.O., Coops N.C., Hilker T., Bater C.W. & Gobakken T., 2012: Lidar sampling for large-area forest characterization: A review. *Remote Sensing of Environment*, 121: 196–209.

Yao W., Krzystek P. & Heurich M., 2012: Tree species classification and estimation of stem volume and DBH based on single tree extraction by exploiting airborne full-waveform LiDAR data. *Remote Sensing of Environment*, 123: 368–380.

Yu X., Hyyppä J., Vastaranta M., Holopainen M. & Viitala R., 2011: Predicting individual tree attributes from airborne laser point clouds based on the random forests technique. *ISPRS Journal of Photogrammetry and Remote Sensing*, 66: 28–37.

Received: 9 January 2020
Accepted: 11 June 2020